AERMOD: A Dispersion Model for Industrial Source Applications.
Part I: General Model Formulation and Boundary Layer Characterization

Alan J. Cimorelli,* Steven G. Perry,[+] Akula Venkatram,[#] Jeffrey C. Weil,[@] Robert J. Paine,[&]
Robert B. Wilson,** Russell F. Lee,[++] Warren D. Peters,[##] and Roger W. Brode[@@]

*U.S. Environmental Protection Agency Region 3, Philadelphia, Pennsylvania
[+]Air Resources Laboratory, NOAA, and National Exposure Research Laboratory, U.S. Environmental Protection Agency,
Research Triangle Park, North Carolina
[#]College of Engineering, University of California, Riverside, Riverside, California
[@]Cooperative Institute for Research in Environmental Sciences, University of Colorado, Boulder, Colorado
[&]ENSR International, Westford, Massachusetts
**U.S. Environmental Protection Agency Region 10, Seattle, Washington
[++]Charlotte, North Carolina
[##]OAQPS, U.S. Environmental Protection Agency, Research Triangle Park, North Carolina
[@@]MACTEC Federal Programs, Inc., Durham, North Carolina

ABSTRACT

The formulation of the American Meteorological Society (AMS) and U.S. Environmental Protection Agency (EPA) Regulatory Model (AERMOD) Improvement Committee's applied air dispersion model is described. This is the first of two articles describing the model and its performance. Part I includes AERMOD's characterization of the boundary layer with computation of the Monin–Obukhov length, surface friction velocity, surface roughness length, sensible heat flux, convective scaling velocity, and both the shear- and convection-driven mixing heights. These parameters are used in conjunction with meteorological measurements to characterize the vertical structure of the wind, temperature, and turbulence. AERMOD's method for considering both the vertical inhomogeneity of the meteorological characteristics and the influence of terrain are explained. The model's concentration estimates are based on a steady-state plume approach with significant improvements over commonly applied regulatory dispersion models. Complex terrain influences are provided by combining a horizontal plume state and a terrain-following state. Dispersion algorithms are specified for convective and stable conditions, urban and rural areas, and in the influence of buildings and other structures. Part II goes on to describe the performance of AERMOD against 17 field study databases.

1. Introduction

Major developments in an improved understanding of the planetary boundary layer (PBL) began in the 1970s (Wyngaard 1988). One milestone involved numerical simulations by Deardorff (1972), revealing the convective boundary layer's (CBL's) vertical structure and important turbulence scales. Insights into dispersion followed from laboratory experiments, numerical simulations, and field observations (Briggs 1988; Lamb 1982; Weil 1988a). For the stable boundary layer (SBL), advancements occurred more slowly. However,

a sound theoretical/experimental framework for surface layer dispersion and approaches for elevated sources existed by the mid-1980s (Briggs 1988; Venkatram 1988).

During the 1980s, researchers began to apply this information to applied dispersion models. These included eddy-diffusion techniques for surface releases, statistical theory and PBL scaling for dispersion parameter estimation, and a new probability density function (PDF) approach for the CBL. Much of this work was reviewed and promoted in workshops (Weil 1985), revised texts (Pasquill and Smith 1983), and in short courses and monographs (Nieuwstadt and van Dop 1982; Venkatram and Wyngaard 1988). By the mid- to late 1980s, new applied dispersion models had been developed, including the Power Plant Siting Program (PPSP) model (Weil and Brower 1984), Second-Order Closure Integrated Puff (SCIPUFF) (Sykes et al. 1996), Operationelle Meteorologiske Luftkvalitetsmodeller

Corresponding author address: Alan J. Cimorelli, U.S. Environmental Protection Agency, Region 3, 1650 Arch Street, Philadelphia, PA 19107.
E-mail: cimorelli.alan@epa.gov

(OML) (Berkowicz et al. 1986), Hybrid Plume Dispersion Model (HPDM) (Hanna and Paine 1989), Multiple Source Dispersion Algorithm Using On-Site Turbulence Data (TUPOS) (Turner et al. 1986), and the Complex Terrain Dispersion Model Plus Algorithms for Unstable Situations (CTDMPLUS) (Perry et al. 1989); later, the Advanced Dispersion Modeling System (ADMS), developed in the United Kingdom (Carruthers et al. 1994), was added as well.

In February 1991, the U.S. Environmental Protection Agency (EPA) in conjunction with the American Meteorological Society (AMS) formed the AMS and EPA Regulatory Model (AERMOD) Improvement Committee (AERMIC), with the purpose of incorporating scientific advances from the 1970s and 1980s into a state-of-the-art dispersion model for regulatory applications. AERMIC's early efforts are described by Weil (1992). To improved PBL parameterizations, other concerns such as plume interaction with terrain, surface releases, building downwash, and urban dispersion were addressed. These efforts resulted in AERMOD. AERMOD is aimed at the same scenarios currently handled by EPA's Industrial Source Complex Short-Term model (ISCST3) (U.S. Environmental Protection Agency 1995). The early formulations of AERMOD are summarized in Perry et al. (1994) and Cimorelli et al. (1996). An extensive discussion of the current models' formulations appears in Cimorelli et al. (2003).

AERMOD, a steady-state dispersion model, includes the effects on dispersion from vertical variations in the PBL. In the SBL the concentration distribution is Gaussian, both vertically and horizontally, as is the horizontal distribution in the CBL. However, the CBL's vertical concentration distribution is described with a bi-Gaussian PDF, as demonstrated by Willis and Deardorff (1981). Buoyant plume mass that penetrates the elevated stable layer is tracked by AERMOD and allowed to reenter the mixed layer at some distance downwind.

For flow in complex terrain, AERMOD incorporates the concept of a dividing streamline (Snyder et al. 1985), and the plume is modeled as a combination of terrain-following and terrain-impacting states. The model considers the influence of building wakes and it enhances vertical turbulence to account for the "convective like" boundary layer found in nighttime urban areas.

This paper describes 1) algorithms for estimating PBL parameters, 2) algorithms for developing vertical meteorological profiles, 3) an approach for handling PBL inhomogeneity, 4) the approach used to establish the influence of terrain, 5) the general structure of the dispersion model, 6) the dispersion algorithms, 7) the building downwash algorithms, and 8) treatment of the urban boundary layer. Perry et al. (2005, hereinafter Part II) discusses the performance evaluation of AERMOD against 17 experimental databases.

2. Meteorological preprocessor (AERMET)

The growth and structure of the PBL is driven by the fluxes of heat and momentum, which, in turn, depend upon surface effects. The depth of this layer and the dispersion of pollutants within it are influenced on a local scale by surface characteristics such as surface roughness, albedo, and available surface moisture. As with models like HPDM (Hanna and Paine 1989; Hanna and Chang 1993) and CTDMPLUS (Perry 1992), AERMOD utilizes surface and mixed-layer scaling to characterize the structure of the PBL. AERMOD's meteorological preprocessor (AERMET) requires, as input, surface characteristics, cloud cover, a morning upper-air temperature sounding, and one near-surface measurement of wind speed, wind direction, and temperature. With this, the model computes the friction velocity, Monin–Obukhov length, convective velocity scale, temperature scale, mixing height, and surface heat flux. In a manner similar to models like CTDMPLUS and HPDM these scaling parameters are used to construct vertical profiles of wind speed, lateral and vertical turbulence, potential temperature gradient, and potential temperature. Extensive independent evaluations of these scaling parameters and vertical profiles have not been performed for urban and complex terrain situations other than those accomplished in the many references sited. However, evaluations of the overall model have shown that these parameterizations lead to estimates of plume concentration that compare well with a wide variety of field observations (Part II).

a. Derived parameters in the CBL

During convective conditions, AERMET characterizes the state of the PBL by first estimating the sensible heat flux (H) with a simple energy balance approach (Oke 1978), then the friction velocity (u_*) and the Monin–Obukhov length (L). With these parameters AERMET can estimate the mixing height (z_i) and the convective velocity scale (w_*).

The expression used for u_* (Panofsky and Dutton 1984) is

$$u_* = \frac{k u_{\text{ref}}}{\ln(z_{\text{ref}}/z_0) - \Psi_m\{z_{\text{ref}}/L\} + \Psi_m\{z_0/L\}}, \quad (1)$$

where k is the von Kármán constant, u_{ref} is the wind speed at reference height, z_{ref} is the lowest surface layer measurement height for wind, z_0 is the roughness length, and Ψ_m is defined by Panofsky and Dutton (1984) for the CBL and by van Ulden and Holtslag (1985) for the SBL. Note that braces are used throughout this paper to denote the functional form of variables. Assuming neutral conditions, u_* and L are initialized using Eq. (1) and L is defined as follows (Wyngaard 1988):

$$L = -\frac{\rho c_p T_{\text{ref}} u_*^3}{kgH}, \tag{2}$$

where g is the acceleration of gravity, c_p is the specific heat at constant pressure, ρ is the density, and T_{ref} is the ambient temperature (K) that is representative of the surface layer. Final values for u_* and L are found by iterating Eqs. (1) and (2) until convergence. The convective velocity scale (w_*) is estimated from (Deardorff 1970)

$$w_* = \left(\frac{gHz_{ic}}{\rho c_p T_{\text{ref}}}\right)^{1/3}, \tag{3}$$

where z_{ic} is the convective mixing height.

Assuming no measurements, z_{ic} is calculated with a simple one-dimensional energy balance model (Carson 1973), as modified by Weil and Brower (1983). In addition, a mechanical mixing height (z_{im}) is estimated from an empirically based expression (Venkatram 1980) as

$$z_{im} = 2300u_*^{3/2}, \tag{4}$$

where the constant 2300 has units of $(\text{s}^{3/2} \text{ m}^{-1/2})$.

For CBL dispersion calculations, the mixing height (z_i) is defined as the larger of z_{im} and z_{ic}.

b. Derived parameters in the SBL

Because estimates of the sensible heat flux using Oke's (1978) approach are unreliable in the SBL, Eqs. (1) and (2) are not used. Rather, using Venkatram's (1980) observation that the temperature scale (θ_*), which sets the "level" of the temperature fluctuations in the surface layer, varies little during the night, u_* can be determined from

$$\theta_* = -H/\rho c_p u_*; \tag{5}$$

$\theta_* = 0.09(1 - 0.5n^2)$ is taken from van Ulden and Holtslag (1985), where n is the fractional cloud cover and the constant 0.09 has units of kelvins.

By combining Eq. (2) with Eq. (5), L can be written as

$$L = \frac{T_{\text{ref}}}{kg\theta_*} u_*^2. \tag{6}$$

Using Panofsky and Dutton's (1984) expression for the wind speed profile, that is,

$$u = \frac{u_*}{k}\left[\ln\left(\frac{z}{z_0}\right) + \frac{\beta_m z_{\text{ref}}}{L}\right], \tag{7}$$

where $\beta_m = 5$, the solution for u_* is found by substituting Eq. (6) into Eq. (7) (Hanna and Chang 1993; Perry 1992).

Having computed u_* and θ_*, AERMET calculates the surface heat flux from Eq. (5). Last, because there is, by definition, no convective component in the SBL,

the total mixing depth z_i is computed as the time-smoothed (Cimorelli et al. 2003) mechanical mixing depth z_{im} [Eq. (4)].

3. Vertical structure of the PBL

AERMOD estimates meteorological profiles using both measurements and similarity parameterizations [i.e., AERMOD uses the shape of the similarity profiles to interpolate between adjacent vertical measurements (Cimorelli et al. 2003)]. AERMOD's concentration formulations consider the effects from vertical variations in wind, temperature, and turbulence. These profiles are represented by equivalent (effective) values constructed by averaging over the layer through which plume material travels directly from the source to receptor (Cimorelli et al. 2003). The effective parameters are denoted by a tilde throughout the document (e.g., effective wind speed is denoted by $\tilde{u}$).

a. Wind speed and direction

The profile equation for wind speed has the familiar logarithmic form:

$$u\{z\} = u\{z = 7z_0\}\left(\frac{z}{7z_0}\right) \qquad \text{for} \qquad z < 7z_0,$$

$$u\{z\} = \frac{u_*}{k}\left[\ln\left(\frac{z}{z_0}\right) - \Psi_m\left\{\frac{z}{L}\right\}\right.$$
$$\left. + \Psi_m\left\{\frac{z_0}{L}\right\}\right] \qquad \text{for} \quad 7z_0 \leq z \leq z_i,$$

and

$$u\{z\} = u\{z = z_i\} \qquad \text{for} \qquad z > z_i, \tag{8}$$

where $7z_0$ represents an approximate height of roughness elements below which the profile is assumed to be linear.

Wind direction is assumed to be constant with height both above the highest and below the lowest measurement and to vary linearly between measurements.

b. Potential temperature gradient

In the CBL $\partial\theta/\partial z$ is taken to be zero, in the stable interfacial layer it is estimated from the morning temperature sounding, and it is assumed to equal 0.005 K m^{-1} above, as suggested by Hanna and Chang (1991). Measurements (e.g., Clarke et al. 1971) of profiles throughout the day lend support to this approach.

In the SBL's first 100 m, $\partial\theta/\partial z$ is estimated from Dyer (1974) and Panofsky and Dutton (1984) as

$$\frac{\partial\theta}{\partial z} = \frac{\theta_*}{k(2)}\left[1 + 5\frac{(z = 2)}{L}\right] \quad \text{for} \qquad z \leq 2 \text{ m}$$

and

$$\frac{\partial \theta}{\partial z} = \frac{\theta_*}{kz}\left(1 + 5\frac{z}{L}\right) \qquad \text{for} \quad 2\text{ m} < z \leq 100\text{ m}.$$

$$(9)$$

Above 100 m the potential temperature gradient is taken from Stull (1983) and van Ulden and Holtslag (1985) as

$$\frac{\partial \theta}{\partial z} = \frac{\partial \theta\{z_{\text{mx}}\}}{\partial z}\exp\left[-\frac{(z - z_{\text{mx}})}{0.44 z_{i\theta}}\right], \qquad (10)$$

where $z_{\text{mx}} = 100$ m, $z_{i\theta} = \max(z_{im}, 100$ m), and the constant 0.44 is taken from measurements (Andre and Mahrt 1982). Last, AERMOD limits $\partial\theta/\partial z$ to a minimum of 0.002 K m^{-1} (Paine and Kendall 1993).

c. Vertical turbulence

In the CBL, vertical turbulence contains both a mechanical ($\sigma_{wm} \propto u_*$) and a convective ($\sigma_{wc} \propto w_*$) component, with the total vertical turbulence (σ_{wT}^2) given by

$$\sigma_{wT}^2 = \sigma_{wc}^2 + \sigma_{wm}^2, \qquad (11)$$

while in the SBL $\sigma_{wT} = \sigma_{wm}$. These forms are similar to one introduced by Panofsky et al. (1977) and are included in other dispersion models (e.g., Berkowicz et al. 1986; Hanna and Paine 1989; and Weil 1988a).

The convective portion (σ_{wc}^2) of the total variance is calculated as

$$\sigma_{wc}^2 = 1.6\left(\frac{z}{z_{ic}}\right)^{2/3} w_*^2 \qquad \text{for} \qquad z \leq 0.1 z_{ic},$$

$$\sigma_{wc}^2 = 0.35 w_*^2 \qquad \text{for} \quad 0.1 z_{ic} < z \leq z_{ic},$$

and

$$\sigma_{wc}^2 = 0.35 w_*^2 \exp\left[-\frac{6(z - z_{ic})}{z_{ic}}\right] \quad \text{for} \qquad z > z_{ic},$$

$$(12)$$

where the first expression is taken from Panofsky et al. (1977) and the second from Hicks (1985). The third expression permits σ_{wc}^2 to smoothly decay to zero well above z_{ic}.

The mechanical turbulence (σ_{wm}) is assumed to consist of contributions from the current boundary layer (σ_{wml}) and residual turbulence from the previous day's boundary layer (σ_{wmr}), such that

$$\sigma_{wm}^2 = \sigma_{wml}^2 + \sigma_{wmr}^2. \qquad (13)$$

The expression for σ_{wml}, following Brost et al. (1982), is

$$\sigma_{wml} = 1.3 u_*\left(1 - \frac{z}{z_i}\right)^{1/2} \quad \text{for} \quad z < z_i$$

and

$$\sigma_{wml} = 0.0 \qquad \text{for} \quad z \geq z_i, \qquad (14)$$

where $\sigma_{wml} = 1.3u_*$ at $z = 0$ is consistent with Panofsky et al. (1977). In the absence of measurements above z_i, σ_{wmr} is taken from (Briggs 1973) to be $0.02u\{z_i\}$.

d. Lateral turbulence

In the CBL the total lateral turbulence is also assumed to be a combination of a mechanical (σ_{vm}) and a convective (σ_{vc}) portion, such that

$$\sigma_{vT}^2 = \sigma_{vc}^2 + \sigma_{vm}^2. \qquad (15)$$

In the mixed layer,

$$\sigma_{vc}^2 = 0.35 w_*^2, \qquad (16)$$

which is supported by the Minnesota (Readings et al. 1974; Kaimal et al. 1976) and Ashchurch, United Kingdom (Caughey and Palmer 1979), datasets. Consistent with measurements reported by Hanna (1983), a minimum value of 0.5 m s^{-1} is assumed for σ_{vc} above z_i.

AERMOD assumes that σ_{vm}^2 varies linearly with height between its value at the surface and an assumed residual value at z_{im} as is suggested by field observations (e.g., Brost et al. 1982). The value of σ_{vm}^2 at z_{im} is assumed to persist at higher levels. The profile for lateral mechanical turbulence is calculated as

$$\sigma_{vm}^2 = \left(\frac{\sigma_{vm}^2\{z_{im}\} - \sigma_{vo}^2}{z_{im}}\right)z + \sigma_{vo}^2 \quad \text{for} \quad z \leq z_{im}$$

and

$$\sigma_{vm}^2 = \sigma_{vm}^2\{z_{im}\} \qquad \text{for} \quad z > z_{im}, \qquad (17)$$

where $\sigma_{vm}^2\{z_{im}\} = \min(\sigma_{vo}^2, 0.25$ m^2 s$^{-2})$ and σ_{vo}^2 is equal to $3.6u_*^2$ (Panofsky and Dutton 1984; Izumi 1971; Hicks 1985). In the SBL the turbulence is exclusively mechanical (σ_{vm}).

4. General form of the AERMOD dispersion model with terrain

AERMOD simulates a plume, in elevated terrain, as a weighted sum of concentrations from two limiting states: a horizontal plume (terrain impacting) and a terrain-following plume. Each plume state is weighted using the concepts of the critical dividing streamline and a receptor-specific terrain height scale (h_c) (Venkatram et al. 2001; Cimorelli et al. 2003).

The general concentration equation is

$$C_T\{x_r, y_r, z_r\} = f C_{c,s}\{x_r, y_r, z_r\} + (1 - f)C_{c,s}\{x_r, y_r, z_p\},$$

$$(18)$$

where $C_T\{x_r, y_r, z_r\}$ is the total concentration, $C_{c,s}\{x_r, y_r, z_r\}$ is the contribution from the horizontal plume (subscripts c and s refer to convective and stable conditions, respectively), $C_{c,s}\{x_r, y_r, z_p\}$ is the contribution from the terrain-following plume, f is the weighting factor, $\{x_r, y_r, z_r\}$ is the receptor coordinate, z_p $(=z_r - z_t)$ is the re-
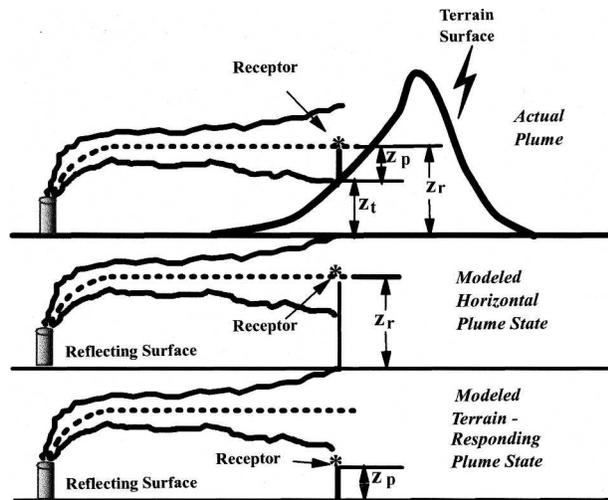
FIG. 1. AERMOD two-state approach. The total concentration predicted by AERMOD is the weighted sum of the two extreme possible plume states: the horizontal plume state and the terrain-following state.

ceptor height above local ground, and z_t is the local terrain height. Figure 1 illustrates the relationship between the actual plume and AERMOD's characterization of it.

The weighting of the two plume states depends on the amount of mass residing in each state. This mass partitioning is based on the relationship between the critical dividing streamline height (H_c) (Sheppard 1956; Snyder et al. 1985) and the vertical concentration distribution at a receptor. Complex terrain in often characterized by a number of irregularly shaped hills. Venkatram et al. (2001) first proposed the idea that H_c could be calculated using a receptor-specific height scale (h_c) that represents the height of a single isolated hill, which would act to affect the flow at the receptor in a manner similar to the real terrain. In this way, the participating of the plume mass into the two states is receptor specific. For a receptor at elevation z_t and an effective plume height of h_e, the height of the terrain-following state, at that receptor, is $z_t + h_e$. For streamlines to reach the terrain-following height the actual terrain that influences the flow at the receptor must extend up to or above this height; in this case, $h_c = z_t + h_e$. If the actual terrain is less than $z_t + h_e$ then h_c is set to the actual terrain height that causes the maximum vertical displacement of the plume above the receptor. Therefore, for any receptor, h_c is defined as the minimum of the highest actual terrain and the terrain-following height at that receptor. The dividing streamline height is computed using the same integral formula found in CTDMPLUS (Perry 1992), with h_c substituted for hill height.

The fraction of the plume mass below H_c (i.e., φ_p) is computed as

$$
\varphi_p = \frac{\int_0^{H_c} C_s\{x_r, y_r, z_r\}\, dz}{\int_0^{\infty} C_s\{x_r, y_r, z_r\}\, dz} . \tag{19}
$$

In convective conditions, $H_c = 0$ and $\varphi_p = 0$.

As described by Venkatram et al. (2001), the plume-state weighting factor f is given by $f = 0.5(1 + \varphi_p)$. When the plume is entirely below H_c ($\varphi_p = 1.0$ and $f = 1.0$) the concentration is determined by the horizontal plume only. When the plume is entirely above the critical dividing streamline height or when the atmosphere is convective, $\varphi_p = 0$ and $f = 0.5$. That is, during convective conditions the concentration at an elevated receptor is the average of the contributions from the two states. As plumes above H_c encounter terrain and are deflected vertically, there is also a tendency for plume material to approach the terrain surface and to spread out around the sides of the terrain. To simulate this, concentration estimates always contain a component from the horizontal state. Evaluation of the model against field observations supports this assumption (Part II). Therefore, under no conditions is the plume allowed to completely approach the terrain-following state. For flat terrain, the contributions from the two states are equal in value and are equally weighted.

5. AERMOD concentration predictions in the SBL

During stable conditions (i.e., stable and neutral stratifications when $L > 0$), AERMOD estimates concentrations from

$$
C_s\{z_r, y_r, z\} = \frac{Q}{\sqrt{2\pi}\tilde{u}\sigma_{zs}} F_y
$$
$$
\times \sum_{m=-\infty}^{\infty} \left\langle \exp\left[-\frac{(z - h_{es} - 2mz_{ieff})^2}{2\sigma_{zs}^2} \right] \right.
$$
$$
\left. + \exp\left[-\frac{(z + h_{es} + 2mz_{ieff})^2}{2\sigma_{zs}^2} \right] \right\rangle, \tag{20}
$$

where z_{ieff} is the effective mechanical mixing height, σ_{zs} is the total vertical dispersion, h_{es} is the plume height (Weil 1988b; Cimorelli et al. 2003), and F_y is the lateral distribution functions.

Above the mechanical mixing layer turbulence is expected to be small. AERMOD is designed with an effective mixing lid z_{ieff} that retards but does not prevent plume material from spreading into this region of low turbulence. When the plume is below z_{im} but its "upper edge" (plume height plus $2.15\sigma_{zs}$) reaches z_{im}, z_{ieff} is allowed to increase, maintaining its position relative to the plume.
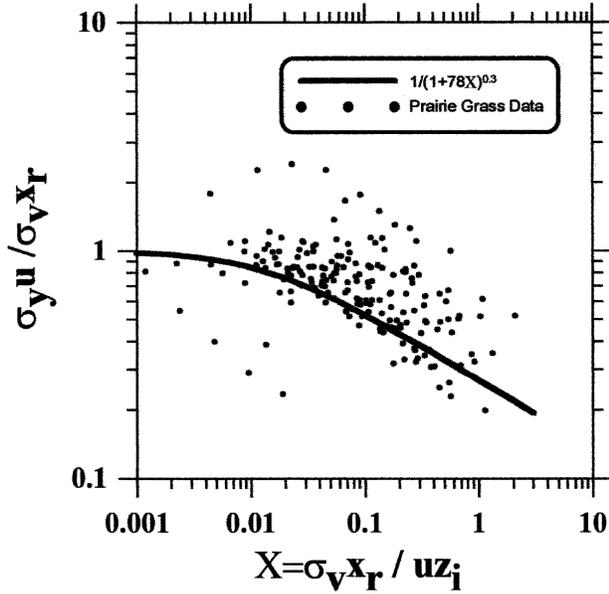
The lateral dispersion function is defined as

FIG. 2. Lateral spread (σ_y) as a function of nondimensional distance (X). The data are taken from the Prairie Grass Experiment (Barad 1958).

$$F_y = \frac{1}{\sqrt{2\pi}\sigma_y} \exp\left(\frac{-y^2}{2\sigma_y^2}\right). \qquad (21)$$

Lateral dispersion is estimated from Taylor (1921), such that

$$\sigma_y = (\tilde{\sigma}_v x/\tilde{u}) \Big/ \left(1 + \frac{x/\tilde{u}}{2T_{Ly}}\right)^p, \qquad (22)$$

where $p = 0.5$, $\tilde{u}$ is the wind speed, $\tilde{\sigma}_v$ is lateral turbulence velocity [Eq. (15)], and T_{Ly} is the Lagrangian integral time scale. Application of Eq. (22) in a preliminary version of AERMOD yielded poor comparisons with data from the Prairie Grass Experiment (Barad 1958); the lateral spread was not well matched. In response, the lateral dispersion expression was reformulated to better fit the data.

From Venkatram et al. (1984) T_{Ly} is written as $l/\tilde{\sigma}_v$, where l is a lateral turbulent length scale. This allows Eq. (22) to be written in terms of the nondimensional downwind distance X and a nondimensional height scale δ:

$$\sigma_y = \frac{\tilde{\sigma}_v x}{\tilde{u}(1 + \delta X)^p}, \qquad (23)$$

where $X = \tilde{\sigma}_v x/\tilde{u}z_i$, and $\delta = z_i/l$.

Using a subset of stable and convective cases from the Prairie Grass Experiment, Eq. (23) (based on Taylor 1921) produced the best σ_y comparisons with δ and p set equal to 78, and 0.3, respectively. In an independent comparison with the full dataset (Fig. 2), Eq. (23) was found to fall within this widely scattered data, yet it

tended toward the lower end of the distribution of measured dispersion. More important, good agreement between AERMOD concentration predictions and Prairie Grass observations was found (Part II).

In the SBL, the vertical dispersion (σ_{zs}) is assumed to be composed of contributions from an elevated (σ_{zes}) and near-surface (σ_{zgs}) component. Lacking a strong physical justification otherwise, for $h_{es} < z_i$, a simple linear interpolation between the two components is assumed. That is,

$$\sigma_{zs} = \left(1 - \frac{h_{es}}{z_i}\right)\sigma_{zgs} + \left(\frac{h_{es}}{z_i}\right)\sigma_{zes}, \qquad (24)$$

where h_{es} is the plume height, and for $h_{es} \geq z_i$, σ_{zs} is set equal to σ_{zes}.

The elevated component follows Taylor, such that

$$\sigma_{zes} = \tilde{\sigma}_{wT}(x/\tilde{u}) \Big/ \left(1 + \frac{x/\tilde{u}}{2T_{Lzs}}\right)^{1/2}, \qquad (25)$$

where $\tilde{\sigma}_{wT}$ is the vertical turbulence due to mechanical mixing [Eq. (11)].

Writing the Lagrangian time scale as $T_{Lzs} = l/\tilde{\sigma}_{wT}$ (Venkatram et al. 1984) and interpolating l ($1/l = 1/l_n + 1/l_s$) between its neutral ($l_n = 0.36h_{es}$) and stable ($l_s = 0.27\tilde{\sigma}_{wT}/N$) limits allows Eq. (25) to be rewritten as

$$\sigma_{zes} = \frac{\tilde{\sigma}_{wT}t}{\left[1 + \frac{\tilde{\sigma}_{wT}t}{2}\left(\frac{1}{0.36h_{es}} + \frac{N}{0.27\tilde{\sigma}_{wT}}\right)\right]^{1/2}}, \qquad (26)$$

where N is the Brunt–Väisälä frequency, that is, the frequency of the particle oscillation about its equilibrium position.

The surface component (σ_{zgs}) is calculated as (Venkatram 1992)

$$\sigma_{zgs} = \sqrt{\frac{2}{\pi}}\left(\frac{u_*x}{\tilde{u}}\right)\left(1 + 0.7\frac{x}{L}\right)^{-1/3}. \qquad (27)$$

In addition to ambient turbulence, plume buoyancy contributes to the total dispersion. Buoyancy-induced dispersion is calculated following Pasquill (1976) and Weil (1988b) as

$$\sigma_b = \frac{0.4\Delta h}{\sqrt{2}}, \qquad (28)$$

where Δh is the stable plume rise above stack top (Cimorelli et al. 2003). Total dispersion is calculated by adding σ_b, in quadrature, to σ_y and also to σ_{zs} (Pasquill and Smith 1983).

6. AERMOD concentration predictions in the CBL

Unlike the SBL, in the CBL (i.e., convective and neutral stratifications when $L < 0$), the vertical velocity (w) distribution is positively skewed and results in a

non-Gaussian vertical concentration distribution (Weil et al. 1997; Lamb 1982) and a general descent of the plume centerline for an elevated nonbuoyant source (Lamb 1982; Weil 1988a). The vertical spread in concentration is modeled using a bi-Gaussian distribution, a good approximation to laboratory convection tank data (Baerentsen and Berkowicz 1984). In contrast, the lateral concentration distribution assumes a Gaussian shape, consistent with the lateral velocity distribution (Lamb 1982).

For buoyant releases AERMOD addresses distance-dependent plume rise. A "direct" source is defined to treat that portion of the plume's mass that is transported directly to the ground, plus all subsequent reflections of this direct mass. For plume segments initially rising in updrafts, an "indirect" or modified-image source is included to address the initial reflection at z_i and all subsequent reflections at $z = 0$ and z_i of this indirect mass. A plume-rise component is added to delay the downward dispersion of the indirect source material from the CBL top; this mimics the tendency of buoyant plumes to remain temporarily near z_i and resist downward mixing. Additionally, a "penetrated" source (above the CBL top) is included to account for material that initially penetrates the elevated inversion while allowing for it to subsequently reentrain into the growing CBL. The fraction f_p of the source material that does not penetrate is

$$f_p = 0 \qquad \text{if} \qquad \Delta h_h < 0.5\Delta h_{eq},$$
$$f_p = 1 \qquad \text{if} \qquad \Delta h_h > 1.5\Delta h_{eq},$$

and

$$f_p = \frac{\Delta h_h}{\Delta h_{eq}} - 0.5 \quad \text{if} \quad 0.5\Delta h_{eq} \le \Delta h_h \le 1.5\Delta h_{eq},$$

(29)

where $\Delta h_h = z_i - h_s$, and h_{eq} is the equilibrium plume rise in a stable environment (Weil et al. 1997).

The total concentration (C_c) in the CBL is found by summing the contribution from the three sources. For the horizontal plume state,

$$C_c\{x_r, y_r, z_r\} = C_d\{x_r, y_r, z_r\} + C_r\{x_r, y_r, z_r\}$$
$$+ C_p\{x_r, y_r, z_r\}, \qquad (30)$$

where C_d, C_r, and C_p are the contributions from the direct, indirect, and penetrated sources, respectively. This three-plume concept is shown schematically in Fig. 3. Similarly, the concentration for the terrain-following state has the form of Eq. (30), but with z_r replaced by z_p.

a. Direct source contribution to concentrations in the CBL

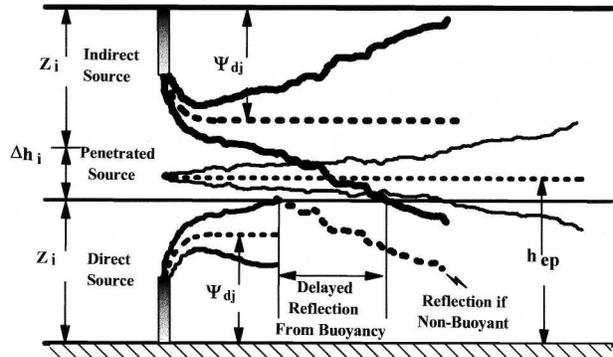Following Weil et al. (1997), the concentration due to the direct plume is given by

FIG. 3. AERMOD's three-plume treatment of the CBL.

$$C_d\{x_r, y_r, z\} = \frac{Q f_p}{\sqrt{2\pi}\tilde{u}} F_y \sum_{j=1}^{2} \sum_{m=0}^{\infty} \frac{\lambda_j}{\sigma_{zj}}$$
$$\times \left\langle \exp\left[-\frac{(z - \Psi_{dj} - 2mz_i)^2}{2\sigma_{zj}^2} \right] \right.$$
$$\left. + \exp\left[-\frac{(z + \Psi_{dj} + 2mz_i)^2}{2\sigma_{zj}^2} \right] \right\rangle, \quad (31)$$

where $\Psi_{dj} = h_s + \Delta h_d + \overline{w}_j x/\tilde{u}$ is the plume height, $\tilde{u}$ is the effective wind speed, F_y [Eq. (21)] is the lateral distribution function, and Δh_d is the plume rise (Briggs 1984). With $z = z_r$ and z_p, Eq. (31) estimates concentrations for the horizontal or terrain-following plume, respectively. The subscript j is equal to 1 for updrafts and 2 for downdrafts with λ_j defined as the weighting coefficient for each distribution. Equation (31) uses an image plume to handle ground reflections by assuming a source at $z = -h_s$. All subsequent reflections are handled by sources at $z = 2z_i + h_s$, $-2z_i - h_s$, $4z_i + h_s$, $-4z_i - h_s$, and so on.

The lateral dispersion coefficient (σ_y), in the equation for F_y, is estimated using the same approach that is used for the SBL [Eqs. (22) and (23)].

The vertical dispersion coefficient (σ_{zj}) is composed of an elevated (σ_{zej}) and surface (σ_{zg}) portion, such that

$$\sigma_{zj}^2 + \sigma_{zej}^2 + \sigma_{zg}^2. \qquad (32)$$

The elevated component is obtained from Weil et al. (1997) as

$$\sigma_{zej} = \alpha_b \frac{\sigma_{wj} x}{\tilde{u}}, \qquad (33)$$

where σ_{wj} is the standard deviation of the updraft ($j = 1$) and downdraft ($j = 2$) distributions of vertical wind speed. The coefficient $\alpha_b = \min(0.6 + 4\Psi_{dj}/z_i, 1.0)$ is designed to be 1.0 above the surface layer ($\psi_{dj} \ge 0.1z_i$) and match Venkatram's (1992) result for a surface source in neutral conditions. For the surface component,

$$\sigma_{zg} = b_c[1 - 10(\Psi_d/z_i)](u_*/\bar{u})^2(x^2/|L|), \quad (34)$$

where $b_c = 0.5$. Above the surface layer, σ_{zg} is set to zero, while for a surface release, Eq. (34) reduces to the form suggested by Venkatram (1992) for vertical dispersion in the unstable surface layer, that is, $\sigma_{zg} \propto (u_*/\bar{u})^2x^2/|L|$. The constant b_c was chosen to provide good agreement between the modeled and observed concentrations for the Prairie Grass Experiment data.

Total lateral and vertical dispersion, for all CBL plumes, are enhanced by plume buoyancy effects in the same manner as described for the SBL [Eq. (28)].

b. Indirect source contribution to concentrations in the CBL

The concentration due to the indirect source is calculated from

$$C_r\{x_r, y_r, z\} = \frac{Qf_p}{\sqrt{2\pi}\bar{u}} F_y \sum_{j=1}^{2} \sum_{m=1}^{\infty} \frac{\lambda_j}{\sigma_{zj}}$$

$$\times \left\langle \exp\left[-\frac{(z + \Psi_{rj} - 2mz_i)^2}{2\sigma_{zj}^2} \right] \right.$$

$$\left. + \exp\left[-\frac{(z - \Psi_{rj} + 2mz_i)^2}{2\sigma_{zj}^2} \right] \right\rangle, \quad (35)$$

where σ_{zj} and F_y are the same as defined for the direct source, the plume height $\psi_{rj} = \psi_{dj} - \Delta h_i$, and Δh_i, which delays vertical mixing to account for residual buoyancy in the plume at the top of the boundary layer, is given by

$$\Delta h_i = \left(\frac{2F_b z_i}{\alpha_h u_p r_y r_z} \right)^{1/2} \frac{x}{u_p}, \quad (36)$$

where r_y and r_z are the plume half-widths in the lateral and vertical directions, u_p is the wind speed used for plume rise, and $\alpha_h = 1.4$ (see Weil et al. 1997).

c. Penetrated source contribution to concentration in the CBL

For the penetrated source, the vertical and lateral concentration distributions have a Gaussian form, such that

$$C_p\{x_r, y_r, z\} = \frac{Q(1 - f_p)}{\sqrt{2\pi}\bar{u}\sigma_{zp}} F_y$$

$$\times \sum_{m=-\infty}^{\infty} \left\langle \exp\left[-\frac{(z - h_{ep} - 2mz_{ieff})^2}{2\sigma_{zp}^2} \right] \right.$$

$$\left. + \exp\left[-\frac{(z + h_{ep} + 2mz_{ieff})^2}{2\sigma_{zp}^2} \right] \right\rangle, \quad (37)$$

where F_y is the same as defined for the SBL and z_{ieff} is the height of the upper reflecting surface in a stable

layer (see section 6). The penetrated plume height $h_{ep} = h_s + \Delta h_{eq}$ for ($f_p = 0$), while for partial penetration $h_{ep} = (h_s + z_i/2) + 0.75\Delta h_{eq}$. The vertical dispersion coefficient (σ_{zp}) contains only a stable elevated component, Eq. (26), because this source is decoupled from the surface. However, for the penetrated source, Eq. (26) is applied with N set to zero because it must pass into or through the well-mixed CBL prior to reaching ground-level receptors.

7. Treatment of lateral plume meander

Plume meander is the slow lateral back-and-forth shifting of the plume in response to nondispersing lateral eddies that are larger than the plume. For time-averaged concentrations, meander has the effect of increasing the lateral spread of the actual plume's distribution. Meander is treated by interpolating the concentrations that result from two limits of the horizontal distribution function (F_y)—the coherent plume limit F_{yC} (which assumes that the wind direction is distributed about a well-defined mean direction) and the random plume limit F_{yR} (which assumes that the plume has equal probability of moving in any direction). The estimated concentration is a weighted sum of the concentrations from these two limits, where the weighting is proportional to the horizontal energy in each of these state.

For the coherent plume, F_{yC} has the familiar Gaussian form

$$F_{yC} = \frac{1}{\sqrt{2\pi}\sigma_y} \exp\left(\frac{-y^2}{2\sigma_y^2} \right), \quad (38)$$

while for the random limit F_{yR} is written as

$$F_{yR} = \frac{1}{2\pi x_r}, \quad (39)$$

where x_r is the straight line distance from the source to the receptor.

To consider meander, the total concentration, on the order of 1 h, for stable or convective conditions ($C_{c,s}$) is determined as a weighted sum of the coherent (C_{Ch}) and random (C_R) plume concentrations as

$$C_{c,s} = C_{Ch}(1 - \sigma_r^2/\sigma_h^2) + C_R(\sigma_r^2/\sigma_h^2); \quad (40)$$

C_{Ch} is computed from Eq. (20) in the SBL and from Eq. (30) in the CBL, with the lateral terms replaced by Eq. (38). Similarly, C_R is computed with the lateral terms replaced by Eq. (39). The weighting factor is the ratio of the random component of the horizontal wind energy (σ_r^2) to the total horizontal wind energy (σ_h^2).

The horizontal wind is composed of a mean component $\bar{u}$, and random components σ_u and σ_v. Thus, a measure of the total horizontal wind "energy" can be represented as

$$\sigma_h^2 = 2\tilde{\sigma}_v^2 + \bar{u}^2, \quad (41)$$

where the mean wind $\bar{u} = (\tilde{u}^2 - 2\tilde{\sigma}_v^2)^{1/2}$. The random component is initially $2\tilde{\sigma}_v^2$ and becomes equal to σ_h^2 at large travel times when the mean wind is uncorrelated, as is seen in the following expression for σ_r^2:

$$\sigma_r^2 = 2\tilde{\sigma}_v^2 + \bar{u}^2[1 - \exp(-x_r/\tilde{u}T_r)], \qquad (42)$$

where T_r is an autocorrelation time scale that is set to 24 h for uncorrelated winds (Brett and Tuller 1991).

8. Building downwash

AERMOD incorporates the Plume Rise Model Enhancements (PRIME) algorithms to handle plumes that are affected by building wakes. A detailed description of PRIME's formulation is found in Schulman et al. (2000). Conceptually, PRIME partitions plume mass between a cavity and wake region according to boundaries that are specified by the lateral and vertical separation streamlines. Dispersion of the mass that is initially captured within the cavity is based on building geometry and is assumed to be uniformly mixed. Beyond the cavity region, this mass is emitted into the wake where it is combined with uncaptured plume mass and dispersed at an enhanced rate (beyond ambient dispersion). In the wake, turbulence smoothly decays with distance, achieving ambient levels in the far field. Plume rise is estimated using a numerical model that includes effects from streamline deflection near the building, vertical wind speed shear, enhanced dilution from the turbulent wake, and velocity deficit.

A basic design tenet for incorporating PRIME into AERMOD was to be as faithful as possible to the PRIME formulation while ensuring that 1) AERMOD's new dispersion regime is applied with PRIME, and 2) far beyond the wake region, concentrations approach AERMOD's estimate. To ensure a smooth transition beyond the wake, the total concentration (C_{total}) is calculated as follows:

$$C_{\text{total}} = \gamma C_{\text{prime}} + (1 - \gamma)C_{\text{AERMOD}}, \qquad (43)$$

where C_{prime} is the concentration that is estimated using the PRIME algorithms with AERMOD-derived meteorological inputs and C_{AERMOD} is the concentration that is estimated using AERMOD without building effects. The weighting parameter γ is designed such that the contribution from the PRIME calculation decreases exponentially with vertical, lateral, and downwind distance from the wake boundaries. That is,

$$\gamma = \exp\left[\frac{-(x - \sigma_{\text{xg}})^2}{2\sigma_{\text{xg}}^2}\right] \exp\left[\frac{-(y - \sigma_{\text{yg}})^2}{2\sigma_{\text{yg}}^2}\right]$$
$$\times \exp\left[\frac{-(z - \sigma_{\text{zg}})^2}{2\sigma_{\text{zg}}^2}\right], \qquad (44)$$

where x is the distance from the upwind edge of the building to the receptor, y is the crosswind distance from the building centerline to the receptor, z is the receptor height above ground, σ_{xg} is the longitudinal dimension of the wake, σ_{yg} is the distance from the building centerline to lateral edge of the wake, and σ_{zg} is the height of the wake at the receptor location, as specified in Schulman et al. (2000).

9. Dispersion characterization in the urban boundary layer

Although urban surface characteristics influence the boundary layer parameters at all times, the thermal effects of the urban area on the structure of the boundary layer is largest at night and relatively absent during the day (Oke 1998). In built-up areas a weak "convective like" boundary layer forms during nighttime hours when stable rural air flows onto a warmer urban surface. AERMOD accounts for this by enhancing the vertical turbulence beyond that found in the nighttime rural boundary layer. A representative convective velocity scale is defined from the urban heat flux (H_u) and urban mixed-layer height (z_{iu}).

Flux H_u is calculated from

$$H_u = \alpha\rho c_p \Delta T_{u-r} u_*, \qquad (45)$$

which is analogous to the bulk transfer parameterization of heat flux over a homogeneous surface (e.g., Businger 1973), with α as the "bulk" transfer coefficient. Because the urban–rural temperature difference ΔT_{u-r} has a maximum value on the order of 10°C, and with light winds u_* on the order of 0.1 m s^{-1}, α should have a maximum value on the order of 0.1 in the city center. Assuming a linear variation of α from 0 at the edge of the urban area to about 0.1 at the center of the urban area results in an areal average of approximately 0.03. This value of α yields very good concentration comparisons between AERMOD and the Indianapolis, Indiana, data (Part II). Here, ΔT_{u-r}, used to estimate H_u, is empirically based on data from Oke (1973, 1982) for a number of Canadian cities with populations from 1000 to 2 000 000. These data were collected during conditions of clear skies, low winds, and low humidities, and represent periods of expected maximum urban effect. An empirical fit to these data yields

$$\Delta T_{u-r} = \Delta T_{\text{max}}[0.1 \ln(P/P_o) + 1.0], \qquad (46)$$

where $\Delta T_{\text{max}} = 12°C$, $P_o = 2\,000\,000$, and P is the population of the modeling domain.

Empirical evidence presented in Oke (1973, 1982) and Venkatram (1978) suggests that $z_{iu} \propto P^{1/4}$, such that

$$z_{iu} = z_{iuo}(P/P_o)^{1/4}, \qquad (47)$$

where z_{iuo} is the boundary layer height corresponding to P_o.

Hanna and Chang (1991) report lidar measurements from the Indianapolis tracer study for nocturnal conditions. While the mixing heights at night range from 100 to 500 m, they were generally around 400 m during

clear, calm conditions. Using 400 m for z_{iu} in Eq. (47), and the Indianapolis population of 700 000, the value of z_{iuo} is computed to be 500 m. This is not inconsistent with measurements by Bornstein (1968) in New York, New York.

The (nighttime urban) convective velocity scale is computed by substituting z_{iu} and H_u into the definitional equation for w_* (Deardorff 1970), such that

$$w_{*u} = \left(\frac{gH_u z_{iuc}}{\rho c_p T_{\mathrm{ref}}} \right)^{1/3}. \tag{48}$$

Enhanced vertical turbulence in the urban boundary layer is computed using Eq. (11) with Eq. (48) used for the convective velocity scale. With enhanced turbulence, vertical dispersion is calculated from Eq. (26).

10. Summary

This paper presents a comprehensive description of the AERMOD dispersion model formulations, including AERMOD's characterization of the boundary layer, the representative terrain used to influence flow, and the specification of model dispersion algorithms for both convective and stable conditions in urban and rural areas. A notable strength of AREMOD's formulations, particularly in the characterization of the boundary layer, lies in its reliance on previously successful modeling approaches that have been established in the literature, coupled with the developers' efforts to avoid major discontinuities that are often found in atmospheric dispersion models. The performance of this model has been evaluated, with results documented in Part II.

REFERENCES

Andre, J. C., and L. Mahrt, 1982: The nocturnal surface inversion and influence of clean-air radiative cooling. *J. Atmos. Sci.,* **39,** 864–878.

Baerentsen, J. H., and R. Berkowicz, 1984: Monte Carlo simula-

tion of plume dispersion in the convective boundary layer. *Atmos. Environ.,* **18,** 701–712.

Barad, M. L., 1958: Project Prairie Grass, A field program in diffusion. Vols. I and II, Geophysical Research Papers No. 59, Air Force Cambridge Research Center, AFCRC-TR-58-235, 439 pp.

Berkowicz, R., J. R. Olesen, and U. Torp, 1986: The Danish Gaussian air pollution model (OLM): Description, test and sensitivity analysis, in view of regulatory applications. *Air Pollution Modeling and Its Application,* V. C. De Wispelaire, F. A. Schiermeier, and N. V. Gillani, Eds., Plemum, 453–481.

Bornstein, R. D., 1968: Observations of urban heat island effects in New York city. *J. Appl. Meteor.,* **7,** 575–582.

Brett, A. C., and S. E. Tuller, 1991: Autocorrelation of hourly wind speed observations. *J. Appl. Meteor.,* **30,** 823–833.

Briggs, G. A., 1973: Diffusion estimation for small emissions. Air Resources Atmospheric Turbulence and Diffusion Laboratory, Environmental Research Laboratory, NOAA, 1973 Annual Rep. ATDL-79, 59 pp.

——, 1984: Plume rise and buoyancy effects. *Atmospheric Science and Power Production,* D. Randerson, Ed., U.S. Department of Energy, 327–366.

——, 1988: Analysis of diffusion field experiments. *Lectures on Air Pollution Modeling,* A. Venkatram and J. C. Wyngaard, Eds., Amer. Meteor. Soc., 63–117.

Brost, R. A., J. C. Wyngaard, and D. H. Lenschow, 1982: Marine stratocumulus layers. Part II: Turbulence budgets. *J. Atmos. Sci.,* **39,** 818–836.

Businger, J. A., 1973: Turbulent transfer in the atmospheric surface layer. *Workshop on Micrometeorology,* D. A. Haugen, Ed., Amer. Meteor. Soc., 67–100.

Carruthers, D. J., and Coauthors, 1994: UK-ADMS: A new approach to modelling dispersion in the Earth's atmospheric boundary layer. *J. Wind Eng. Indust. Aerodyn.,* **52,** 139–153.

Carson, D. J., 1973: The development of a dry inversion-capped convectively unstable boundary layer. *Quart. J. Roy. Meteor. Soc.,* **99,** 450–467.

Caughey, S. J., and S. G. Palmer, 1979: Some aspects of turbulence structure through the depth of the convective boundary layer. *Quart. J. Roy. Meteor. Soc.,* **105,** 811–827.

Cimorelli, A. J., S. G. Perry, R. F. Lee, R. J. Paine, A. Venkatram, J. C. Weil, and R. B. Wilson, 1996: Current progress in the AERMIC model development program. Preprints, *89th Annual Meeting Air and Waste Management Association,* Pittsburgh, PA, Air and Waste Management Association, 1–27.

——, ——, A. Venkatram, J. C. Weil, R. J. Paine, R. B. Wilson, R. F. Lee, and W. D. Peters, 2003: AERMOD description of model formulation. U.S. Environmental Protection Agency, EPA Rep. 454/R-03-002d, 85 pp.

Clarke, R. H., A. J. Dyer, R. R. Brook, D. G. Reid, and A. J. Troop, 1971: The Wangara experiment: Boundary layer data. Division of Meteorological Physics CSIRO Tech. Rep. 19, 358 pp.

Deardorff, J. W., 1970: Convective velocity and temperature scales for the unstable boundary layer for Rayleigh convection. *J. Atmos. Sci.,* **27,** 1211–1213.

——, 1972: Numerical investigation of neutral and unstable planetary boundary layers. *J. Atmos. Sci.,* **29,** 91–115.

Dyer, A. J., 1974: A review of flux-profile relationships. *Bound.-Layer Meteor.,* **7,** 363–372.

Hanna, S. R., 1983: Lateral turbulence intensity and plume meandering during stable conditions. *J. Appl. Meteor.,* **22,** 1424–1430.

——, and R. J. Paine, 1989: Hybrid Plume Dispersion Model

(HPDM) development and evaluation. *J. Appl. Meteor.,* **28,** 206–224.

——, and J. S. Chang, 1991: Analysis of urban boundary layer data. Vol. III, Modification of the Hybrid Plume Dispersion Model (HPDM) for Urban Conditions and Its Evaluation Using the Indianapolis Data Set, Electric Power Research Institute Project RP-02736-1, 131 pp.

——, and ——, 1993: Hybrid Plume Dispersion Model (HPDM), improvements and testing at three field sites. *Atmos. Environ.,* **27A,** 1491–1508.

Hicks, B. B., 1985: Behavior of turbulent statistics in the convective boundary layer. *J. Climate Appl. Meteor.,* **24,** 607–614.

Izumi, Y., 1971: Kansas 1968 Field Program data report. Air Force Cambridge Research Laboratory, No. 379, AFCRL-72-0041, 79 pp.

Kaimal, J. C., J. C. Wyngaard, D. A. Haugen, O. R. Cote, Y. Izumi, S. J. Caughey, and C. J. Readings, 1976: Turbulence structure in the convective boundary layer. *J. Atmos. Sci.,* **33,** 2152–2169.

Lamb, R. G., 1982: Diffusion in the convective boundary layer. *Atmospheric Turbulence and Air Pollution Modelling,* F. T. M. Nieuwstadt and H. van Dop, Eds., Reidel, 159–229.

Nieuwstadt, F. T. M., and H. van Dop, 1982: *Atmospheric Turbulence and Air Pollution Modelling.* Reidel, 358 pp.

Oke, T. R., 1973: City size and the urban heat island. *Atmos. Environ.,* **7,** 769–779.

——, 1978: *Boundary Layer Climates.* John Wiley and Sons, 372 pp.

——, 1982: The energetic basis of the urban heat island. *Quart. J. Roy. Meteor. Soc.,* **108,** 1–24.

——, 1998: An algorithmic scheme to estimate hourly heat island magnitude. Preprints, *Second Urban Environment Symp.,* Albuquerque, NM, Amer. Meteor. Soc., 80–83.

Paine, R. J., and S. B. Kendall, 1993: Comparison of observed profiles of winds, temperature, and turbulence with theoretical results. Preprints, *Joint Conf. of the American Meteorological Society and Air and Waste Management Association Specialty Conf.: The Role of Meteorology in Managing the Environment in the 90s,* Scottsdale, AZ, Air and Waste Management Association, Publication VIP-29, 395–413.

Panofsky, H. A., and J. A. Dutton, 1984: *Atmospheric Turbulence: Models and Methods for Engineering Applications.* John Wiley and Sons, 417 pp.

——, H. Tennekes, D. H. Lenschow, and J. C. Wyngaard, 1977: The characteristics of turbulent velocity components in the surface layer under convective conditions. *Bound.-Layer Meteor.,* **11,** 355–361.

Pasquill, F., 1976: Atmospheric dispersion parameters in Gaussian plume modeling—Part III: Possible requirements for change in the Turner's Workbook values. U.S. Environmental Protection Agency Rep. EPA-600/4-76-030B, 53 pp.

——, and F. R. Smith, 1983: *Atmospheric Diffusion.* John Wiley and Sons, 440 pp.

Perry, S. G., 1992: CTDMPLUS: A dispersion model for sources in complex topography. Part I: Technical formulations. *J. Appl. Meteor.,* **31,** 633–645.

——, and Coauthors, 1989: Model description and user instructions. Vol. 1, User's Guide to the Complex Terrain Dispersion Model Plus Algorithms for Unstable Situations (CTDMPLUS), U.S. Environmental Protection Agency Rep. EPA/600/8-89/041, 196 pp.

——, A. J. Cimorelli, R. F. Lee, R. J. Paine, A. Venkatram, J. C. Weil, and R. B. Wilson, 1994: AERMOD: A dispersion model for industrial source applications. Preprints, *87th Annual Meeting of the Air and Waste Management Association,* Pittsburgh, PA, Air and Waste Management Association, Publication 94-TA2.3.04, 16 pp.

——, ——, J. C. Weil, A. Venkatram, R. J. Paine, R. B. Wilson, R. F. Lee, and W. D. Peters, 2005: AERMOD: A dispersion model for industrial source applications. Part II: Model performance against seventeen field-study databases. *J. Appl. Meteor.,* **44,** 694–708.

Readings, C. J., D. A. Haugen, and J. C. Kaimal, 1974: The 1973 Minnesota atmospheric boundary layer experiment. *Weather,* **29,** 309–312.

Schulman, L. L., D. G. Strimaitis, and J. S. Scire, 2000: Development and evaluation of the PRIME plume rise and building downwash model. *J. Air Waste Manage. Assoc.,* **50,** 378–390.

Sheppard, P. A., 1956: Airflow over mountains. *Quart. J. Roy. Meteor. Soc.,* **82,** 528–529.

Snyder, W. H., R. S. Thompson, R. E. Eskridge, R. E. Lawson, I. P. Castro, J. T. Lee, J. C. R. Hunt, and Y. Ogawa, 1985: The structure of the strongly stratified flow over hills: Dividing streamline concept. *J. Fluid Mech.,* **152,** 249–288.

Stull, R. B., 1983: A heat flux history length scale for the nocturnal boundary layer. *Tellus,* **35A,** 219–230.

Sykes, R. I., D. S. Henn, and S. F. Parker, 1996: SCIPUFF—A generalized hazard dispersion model. Preprints, *Ninth Joint Conf. on Applications of Air Pollution Meteorology with AWMA,* Atlanta, GA, Amer. Meteor. Soc., 184–188.

Taylor, G. I., 1921: Diffusion by continuous movements. *Proc. London Math. Soc. Ser.,* **2** (20), 196–211.

Turner, D. B., T. Chico, and J. Catalano, 1986: TUPOS—A multiple source Gaussian dispersion algorithm using on-site turbulence data. U.S. Environmental Protection Agency Rep. EPA/600/8-86/010, 39 pp.

U.S. Environmental Protection Agency, 1995: User instructions. Vol. 1, User's Guide for the Industrial Source Complex (ISC3) Dispersion Models (revised), Environmental Protection Agency Rep. EPA-454/b-95-003a, 390 pp.

van Ulden, A. P., and A. A. M. Holtslag, 1985: Estimation of atmospheric boundary layer parameters for diffusion applications. *J. Climate Appl. Meteor.,* **24,** 1196–1207.

Venkatram, A., 1978: Estimating the convective velocity scale for diffusion applications. *Bound.-Layer Meteor.,* **15,** 447–452.

——, 1980: Estimating the Monin-Obukhov length in the stable boundary layer for dispersion calculations. *Bound.-Layer Meteor.,* **19,** 481–485.

——, 1988: Dispersion in the stable boundary layer. *Lectures on Air Pollution Modeling,* A. Venkatram and J. C. Wyngaard, Eds., Amer. Meteor. Soc., 229–265.

——, 1992: Vertical dispersion of ground-level releases in the surface boundary layer. *Atmos. Environ.,* **26A,** 947–949.

——, and J. C. Wyngaard, Eds., 1988: *Lectures on Air Pollution Modeling.* Amer. Meteor. Soc., 390 pp.

——, D. G. Strimaitis, and D. Dicristofaro, 1984: A semiemperical model to estimate vertical dispersion of elevated releases in the stable boundary layer. *Atmos. Environ.,* **18,** 923–928.

——, and Coauthors, 2001: A complex terrain dispersion model for regulatory applications. *Atmos. Environ.,* **35,** 4211–4221.

Weil, J. C., 1985: Updating applied diffusion models. *J. Climate Appl. Meteor.,* **24,** 1111–1130.

——, 1988a: Dispersion in the convective boundary layer. *Lectures on Air Pollution Modeling,* A. Venkatram and J. C. Wyngaard, Eds., Amer. Meteor. Soc., 167–227.

——, 1988b: Plume rise. *Lectures in Air Pollution Modeling,* A. Venkatram and J. C. Wyngaard, Eds., Amer. Meteor. Soc., 119–162.

——, 1992: Updating the ISC model through AERMIC. Preprints,

85th Annual Meeting of Air and Waste Management Association, Pittsburgh, PA, Air and Waste Management Association, Publication 92-100.11, 14 pp.

——, and R. P. Brower, 1983: Estimating convective boundary layer parameters for diffusion applications. Maryland Power Plant Siting Program, Maryland Department of Natural Resources Rep. PPSP-MD-48, 45 pp.

——, and ——, 1984: An updated gaussian plume model for tall stacks. *J. Air Pollut. Control Assoc.,* **34,** 818–827.

——, L. A. Corio, and R. P. Brower, 1997: A PDF dispersion model for buoyant plumes in the convective boundary layer. *J. Appl. Meteor.,* **36,** 982–1003.

Willis, G. E., and J. W. Deardorff, 1981: A laboratory study of dispersion in the middle of the convectively mixed layer. *Atmos. Environ.,* **15,** 109–117.

Wyngaard, J. C., 1988: Structure of the PBL. *Lectures on Air Pollution Modeling,* A. Venkatram and J. C. Wyngaard, Eds., Amer. Meteor. Soc., 9–57.